Internal Medicine
The Japanese Society of Internal Medicine
doi: 10.2169/internalmedicine.1156-18
Intern Med 58: 1157-1162, 2019
http://internmed.jp

【 CASE REPORT 】

Metastatic Malignant Lymphoma Mimicking Cerebral Toxoplasmosis with the "Target Sign"

Hiroki Ueno[1], Kazumi Norose[2], Teppei Kamimura[1], Keichiro Mihara[3], Fumiyuki Yamasaki[4], Kenji Hikosaka[2], Vishwa J. Amatya[5], Yukio Takeshima[5], Kaoru Kurisu[4] and Hirofumi Maruyama[1]

Abstract:

We herein report the case of a 60-year-old man with a "target sign" in the left frontal lobe on magnetic resonance imaging (MRI), which is thought to be a specific sign of cerebral toxoplasmosis. ^{18}F-fluorodeoxyglucose-positron emission tomography showed no increased uptake, and ^{201}Tl-single photon emission computed tomography showed the focal uptake in the left frontal lesion. On a brain biopsy, the patient was given a definitive diagnosis of brain metastasis from diffuse large B-cell lymphoma, and cerebral toxoplasmosis was excluded. In the present case, multilayer intensities on MRI may reflect the fast-growing nature of this tumor.

Key words: target sign, MRI, ^{18}F-FDG PET, ^{201}Tl-SPECT, cerebral toxoplasmosis, malignant lymphoma

(Intern Med 58: 1157-1162, 2019)
(DOI: 10.2169/internalmedicine.1156-18)

Introduction

In general, the "target sign" on magnetic resonance imaging (MRI) is considered a pathognomonic finding for cerebral toxoplasmosis (1, 2). This target sign in cerebral toxoplasmosis has been shown to be divided into two findings: an "eccentric target sign" and a "concentric target sign". The "eccentric target sign" on contrast-enhanced T1-weighted imaging (CE-T1WI) has been considered highly suggestive of cerebral toxoplasmosis with 95% specificity, although this sign is observed in less than 30% of cases of cerebral toxoplasmosis (1, 2). More recently, the "concentric target sign" on T2-weighted imaging (T2WI), which has alternating concentric layers of T2-weighted hypo- and hyperintensities, has been considered even more specific for cerebral toxoplasmosis (3, 4). However, in the daily clinical setting, it is often difficult to differentiate central nervous system (CNS) diseases that show a "target sign" on conventional MRI examinations, as "target signs" in cerebral toxoplasmosis, CNS lymphoma, primary and metastatic CNS tumors, and other intracranial infections, such as tuberculoma or abscesses, closely mimic each other (4).

Therefore, several studies have explored the utility of other diagnostic neuroimaging modalities to differentiate these diseases, such as ^{201}Tl-single-photon emission computed tomography (^{201}Tl-SPECT) (5, 6), ^{18}F-fluorodeoxyglucose-positron emission tomography (^{18}F-FDG PET) (7), and ^{1}H-magnetic resonance spectroscopy (^{1}H-MRS) (8). However, few studies have focused on the discrimination of these diseases, and the findings were not sufficiently conclusive.

We herein report a patient who was initially suspected of having cerebral toxoplasmosis based on a "target sign" on MRI and the absence of an abnormal accumulation on ^{18}F-FDG PET. After ^{201}Tl-SPECT revealed an abnormal accumu-

[1]Department of Clinical Neuroscience and Therapeutics, Graduate School of Biomedical and Health Sciences, Hiroshima University, Japan, [2]Department of Infection and Host Defense, Graduate School of Medicine, Chiba University, Japan, [3]Department of Hematology and Oncology, Research Institute for Radiation Biology and Medicine, Hiroshima University, Japan, [4]Department of Neurosurgery, Graduate School of Biomedical and Health Sciences, Hiroshima University, Japan and [5]Department of Pathology, Graduate School of Biomedical and Health Sciences, Hiroshima University, Japan

Received: March 8, 2018; Accepted: September 18, 2018; Advance Publication by J-STAGE: December 18, 2018
Correspondence to Dr. Hiroki Ueno, hirokiueno@hiroshima-u.ac.jp

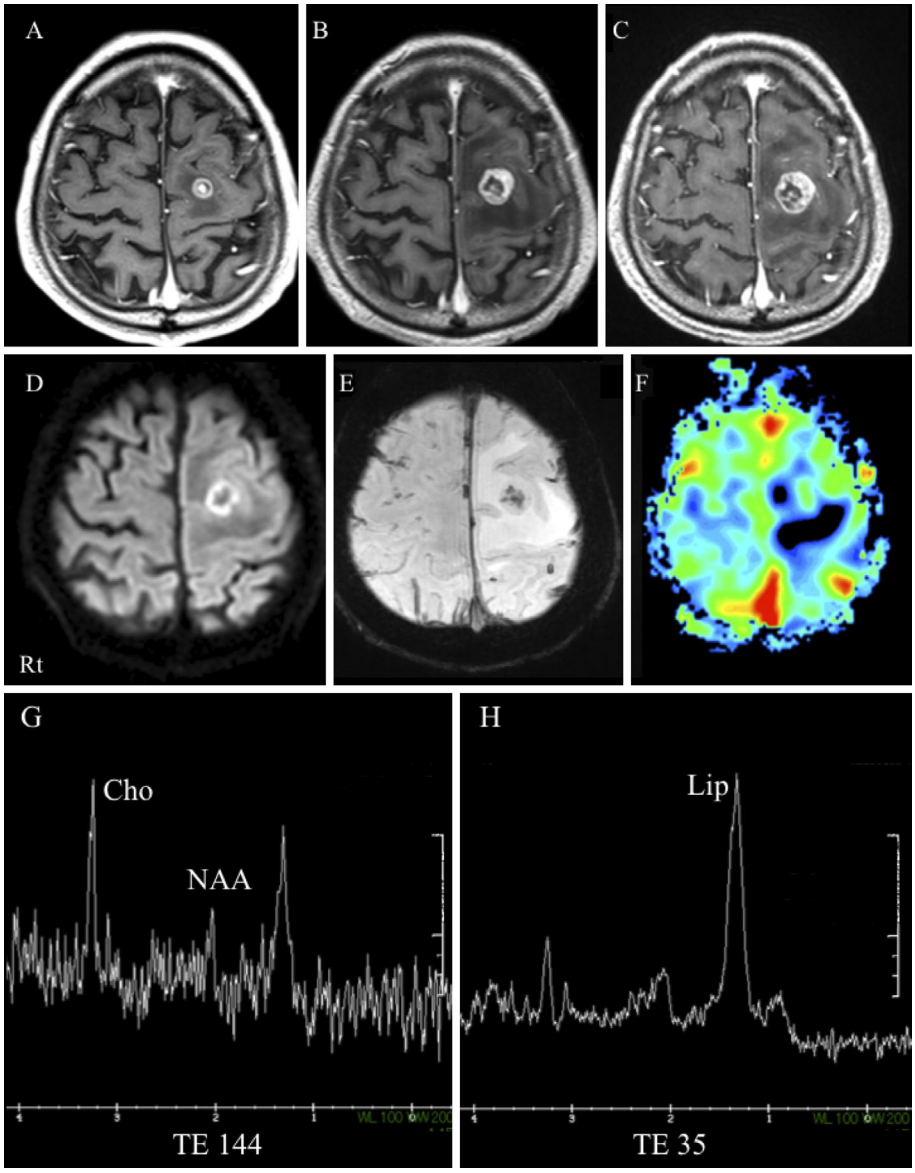

Figure 1. **(A-C) Longitudinal "eccentric target sign" on contrast-enhanced 3D T1-weighted imaging (CE-3D-T1WI). Axial CE-3D-T1WI shows ring enhancement with a small eccentric nodule in the left superior frontal gyrus on imaging performed (A) four days before the onset of the neurological symptoms, (B) on day 11, and (C) on day 19. (D-H) Follow-up multimodal magnetic resonance study performed at admission and on day 11. (D) Diffusion-weighted imaging (*b*-value, 1,000 s/mm^2) showing a high signal intensity in the surrounding wall. (E) Susceptibility-weighted imaging showing punctate hypo-intensities inside a mass lesion. (F) Arterial spin labeling cerebral blood flow maps showing a decreased signal intensity in the left frontal lesion. (G, H) ^{1}H-magnetic resonance spectroscopy (MRS) was performed using the GE technique PROBE with PRESS. ^{1}H-MRS showed a substantially reduced N-acetylaspartate (NAA) peak and an elevated choline (Cho) peak when a long echo time (TE) of 144 ms was used (G) and an elevated lipid (Lip) peak when a short echo time of 35 ms was used (H).**

lation, this patient was given a definitive diagnosis of brain metastasis from diffuse large B-cell lymphoma (DLBCL) based on a brain biopsy.

Case Report

A 60-year-old man who had undergone eight cycles of rituximab, cyclophosphamide, vincristine, doxorubicin, and prednisolone chemotherapy because of a medical history of DLBCL presented with right hemiparesis (day 1). Images from ^{18}F-FDG PET performed two weeks before the onset of the neurological symptoms showed increased metabolism only in the left supraclavicular fossa, with no increased ^{18}F-FDG uptake in the brain. Contrast-enhanced 3D T1-weighted imaging [CE-3D-T1WI; 3D fast-spoiled gradient-recalled echo acquisition in steady state (3D-SPGR), Signa

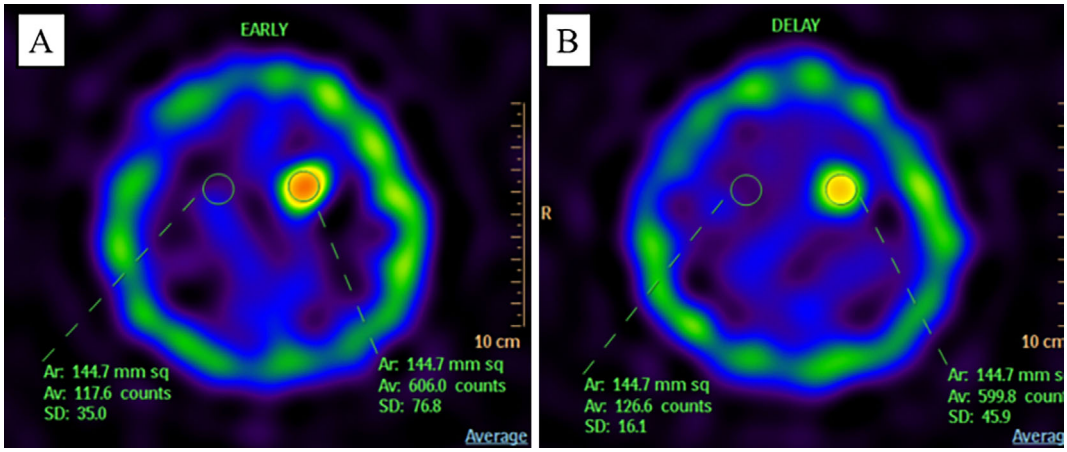

Figure 2. **^{201}Tl-SPECT study performed on day 15. (A) Early ^{201}Tl-SPECT imaging showing a high uptake of radioactivity in the lesion. (B) Delayed ^{201}Tl-SPECT imaging showing a slightly lower uptake of radioactivity in the same area as in (A). Retention index=0.9.**

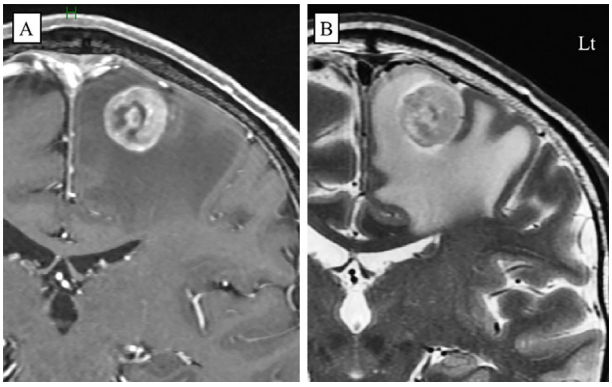

Figure 3. **Follow-up MRI performed on day 19. (A) Coronal CE-3D-T1WI showing a thickened surrounding wall and small papillary-shaped nodule with gadolinium enhancement located inward. (B) Coronal T2WI showing the appearance of multiple layers of alternate hyper-, iso-, and hypo-intensities (i.e., the concentric target sign).**

Excite HD 3.0T; GE Medical Systems, (Milwaukee, USA)] performed four days before the onset of the neurological symptoms showed ring enhancement with a small eccentric nodule in the left superior frontal gyrus, with edema (Fig. 1A). This asymmetric lesion showed the "eccentric target sign" on CE-T1WI. The patient's right hemiparesis worsened, and he was admitted to our hospital on day 8.

The patient was alert and oriented, and his speech was clear and fluent. A neurological examination only revealed weakness, slightly brisk deep tendon reflexes without pathological reflexes in the upper and lower limbs on the right side (muscle bulk and tone were normal. Strength: deltoid 5/5, biceps 4/5, triceps 4/5, wrist extension 4/5, finger abduction 4/5, hip flexion 5/5, hip extension 5/5, knee flexion 4/5, knee extension 4/5, ankle flexion 4/5, ankle extension 4/5), and no signs of sensory disturbance. The white blood cell count was 2.71×10^{3}/μL ($CD4^{+}$ lymphocyte: 1,535/μL, $CD8^{+}$ lymphocyte: 561/μL). Serum human immunodeficiency virus antibodies were negative. Anti-*Toxoplasma* IgG and IgM antibodies in the serum and cerebrospinal fluid (CSF) were negative. The levels of serum C-reactive protein, serum soluble interleukin-2 receptor (sIL-2R), and CSF sIL-2R were 0.10 mg/dL, 564 U/mL, and below 50 U/mL, respectively. CSF cytology revealed no evidence of malignant cells. A flow cytometric analysis and T-cell receptor gene and immunoglobulin heavy chain gene rearrangement analyses of the cells in CSF were not performed. Other laboratory data showed normal findings for blood and CSF.

Follow-up MRI was performed on day 11. CE-3D-T1WI showed enlargement of the lesion in the left frontal lobe (Fig. 1B), and diffusion-weighted imaging showed high signal in the surrounding wall (Fig. 1D). Susceptibility-weighted imaging (SWI) showed punctate hypo-intensities in the inside of a mass lesion (Fig. 1E). Arterial spin labeling cerebral blood flow (CBF) maps showed a decreased signal intensity in the left frontal lesion (Fig. 1F). ^{1}H-MRS using a long echo time showed a reduced N-acetylaspartate peak and an elevated choline peak (Fig. 1G), while with a short echo time, it showed an elevated lipid peak (Fig. 1H). The lack of an increased uptake of ^{18}F-FDG or increased CBF and the presence of the "eccentric target sign" on CE-T1WI, which is highly suggestive of cerebral toxoplasmosis, were findings atypical of malignant lymphoma. Thus, the patient was initially given a provisional diagnosis of cerebral toxoplasmosis and administered sulfamethoxazole/trimethoprim for seven days.

However, the MRI findings and clinical manifestations deteriorated despite treatment. ^{201}Tl-SPECT performed on day 15 revealed a high radiotracer uptake in the lesion (Fig. 2). Following this treatment, another MRI study was performed on day 19. CE-3D-T1WI showed thickening of the surrounding wall (Fig. 1C, 3A) and an enhanced vessel entering a small papillary-shaped nodule located inward (Fig. 3A). T2WI showed a mass lesion accompanied by multiple layers of varying intensity, i.e., the "concentric target sign" (Fig. 3B). Nested-polymerase chain reaction (PCR) tests for *Toxoplasma gondii* 18S rDNA (9) in the CSF and

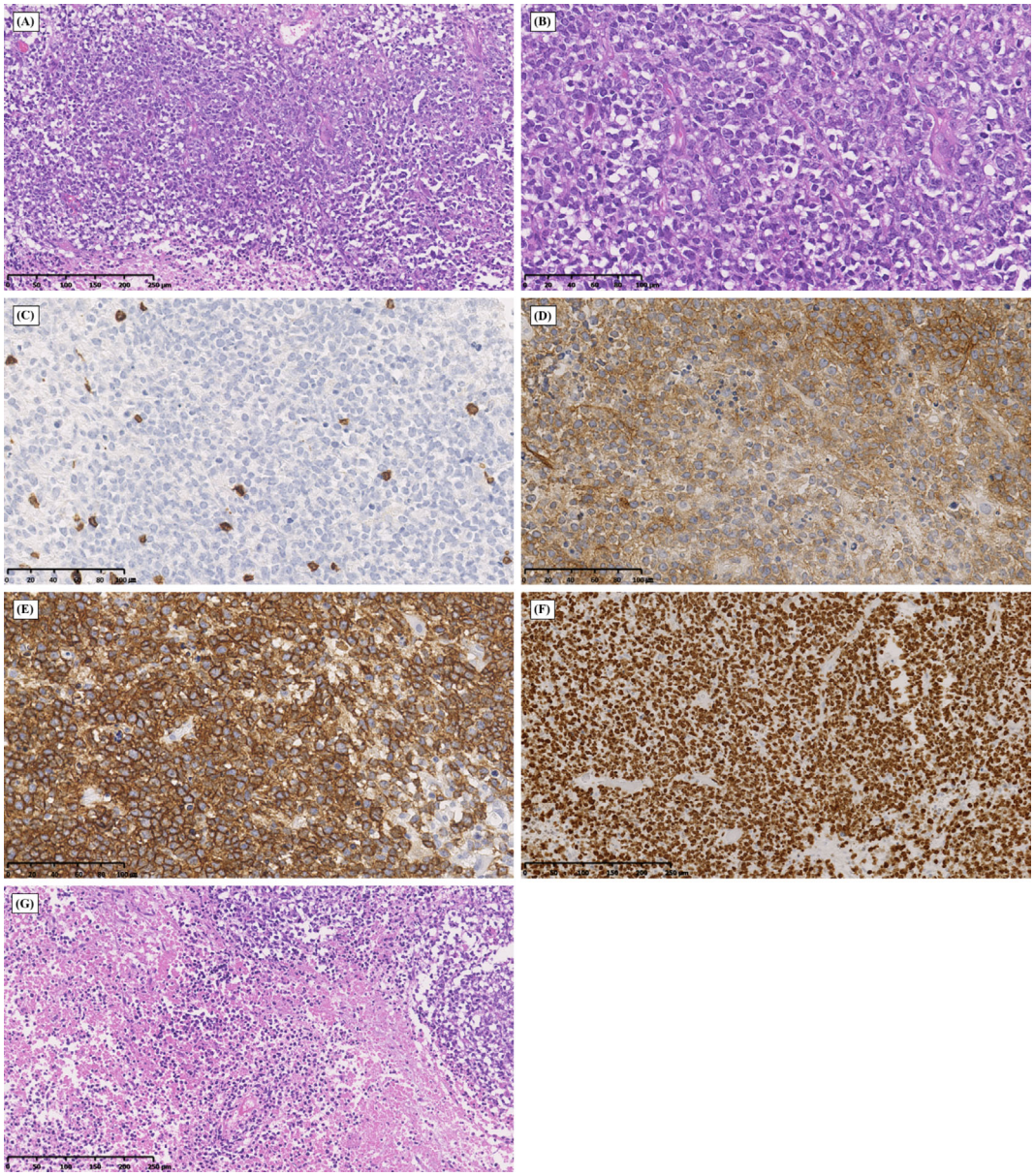

Figure 4. **Histological and immunohistochemical findings from the frontal lobe biopsy. (A) Diffuse proliferation of atypical lymphocytes is present [Hematoxylin and Eosin (H&E) staining]. (B) The tumor cells are large with hyperchromatic nuclei and scant cytoplasm (H&E staining). (C) The atypical cells are negative for CD3 (Immunohistochemical staining). (D) The atypical cells are positive for CD10 (Immunohistochemical staining). (E) The atypical cells are positive for CD20 (Immunohistochemical staining). (F) Ki-67 labeling index is more than 90% (Immunohistochemical staining). (G) Broad areas of necrosis are visible (H&E staining). Scale bars: 250 μm (A, F, G); 100 μm (B-E).**

peripheral blood were negative, and a serological analysis again revealed negative findings of IgG and IgM antibodies for *Toxoplasma*. On day 22, a brain biopsy revealed a metastatic brain tumor comprising DLBCL with large necrotic lesions (Fig. 4). A nested-PCR test for *T. gondii* on the brain biopsy sample was also negative.

The patient's conditions partly improved after high-dose methotrexate with rituximab and radiation therapies.

Discussion

Positive findings of serological IgM and IgG antibodies and PCR for *T. gondii* in peripheral blood, serum, and CSF samples have a high specificity for the diagnosis of toxoplasmosis (10). However, the accurate diagnosis of acute cerebral toxoplasmosis is often difficult without positive laboratory findings. Porter et al. (11) reported that 20% cases of AIDS-related CNS toxoplasmosis were seronegative for *Toxoplasma*. As the serological test for *T. gondii* was negative in this case, it was difficult to diagnose.

When serological and CSF tests show negative findings for *Toxoplasma*, several imaging studies are relied upon for the diagnosis. Regarding toxoplasmosis, two features are considered to be pathognomonic: the "eccentric target sign"

on CE-T1WI and the "concentric target sign" on T2WI. The central enhancing core of the "eccentric target sign" seen on CE-T1WI is produced by a thickened vessel traversing a sulcus. The peripheral enhancing rim is produced by a wall composed of histiocytes and proliferating blood vessels with impaired permeability (2). The "concentric target sign" on T 2WI is a recently described indication of cerebral toxoplasmosis and more specific for toxoplasmosis (3, 4) than tuberculoma (4). It consists of concentric alternating zones of hypo-, hyper-, and iso-intensities. It is thought that T2 hypo-, hyper-, and iso-intensities correspond to zones of hemorrhaging, fibrin-rich necrosis with edema, and compact coagulative necrosis, respectively (4). In cerebral tuberculomas, the "target sign" on T2WI has been reported to be consisted of two zones with hypo-/hyper- intensities and was extremely rare (12, 13). Wasay et al. reported that target-like lesions were seen in only 2% of 100 cases with intracranial tuberculoma (14). In Baló's concentric sclerosis, one or more concentrically multilayered lesions are shown (15). In our case, the findings on other MRI modalities and radioisotope examinations provided little evidence of Baló's concentric sclerosis. Our present case showed hemorrhaging and extensive necrosis on SWI and histopathology, respectively. These findings can be seen in both lymphoma and toxoplasmosis and might have reflected the rapid disease progression. In fact, our present patient was afflicted with metastatic lymphoma, not toxoplasmosis. These results indicate that the MRI findings for metastatic lymphoma can also show an appearance similar to the "concentric target sign" on T2WI of toxoplasmosis.

In situations where it is difficult to differentiate intracranial neoplasms such as lymphoma from non-neoplastic diseases such as toxoplasmosis on MRI, a combination of various imaging modalities should be used to perform a differential diagnosis. Several studies have evaluated the use of ^{201}Tl-SPECT for this purpose (5, 6); an increased focal ^{201}Tl uptake suggests lymphoma, and no ^{201}Tl uptake in the lesion suggests toxoplasmosis. However, Licho et al. reported that the sensitivity and specificity of ^{201}Tl-SPECT for lymphoma are 60% and 55%, respectively, with an accuracy of 57% (16). Thus, in some cases, ^{201}Tl-SPECT may be unreliable for differentiating lymphoma from non-lymphoma. The case described here showed the uptake of ^{201}Tl, which led to the decision to perform a brain biopsy.

Primary CNS lymphoma shows a very high cellular density and increased glucose metabolism and usually shows a strong uptake of ^{18}F-FDG in the tumor. In contrast, Rohren et al. reported that only 61% of cerebral metastatic lesions found on MRI were detected on ^{18}F-FDG-PET (17). Size was a statistically significant factor influencing lesion detection on PET. The average diameter of MRI-detected lesions that went undetected on PET was 0.7 cm (range, 0.2-1.3 cm) (17). In our case, ^{18}F-FDG-PET was performed before the onset of neurological symptoms with negative findings. Therefore, the cerebral lesion might have been too small to detect. Follow-up ^{18}F-FDG-PET was not performed after the onset of the neurological symptoms.

Differentiating lymphoma from non-neoplastic lesions can be difficult, as both conditions may appear clinically and radiologically similar. Studies including a large series of cases and the development of a novel neuroimaging modality for the differential diagnosis are needed to obviate the need for a brain biopsy.

The authors state that they have no Conflict of Interest (COI).

References

1. Ramsey RG, Gean AD. Neuroimaging of AIDS. I. Central nervous system toxoplasmosis. Neuroimaging Clin N Am **7**: 171-186, 1997.
2. Kumar GG, Mahadevan A, Guruprasad AS, et al. Eccentric target sign in cerebral toxoplasmosis: neuropathological correlate to the imaging feature. J Magn Reson Imaging **31**: 1469-1472, 2010.
3. Masamed R, Meleis A, Lee EW, Hathout GM. Cerebral toxoplasmosis: case review and description of a new imaging sign. Clin Radiol **64**: 560-563, 2009.
4. Mahadevan A, Ramalingaiah AH, Parthasarathy S, Nath A, Ranga U, Krishna SS. Neuropathological correlate of the "concentric target sign" in MRI of HIV-associated cerebral toxoplasmosis. J Magn Reson Imaging **38**: 488-495, 2013.
5. Ruiz A, Ganz WI, Post MJ, et al. Use of thallium-201 brain SPECT to differentiate cerebral lymphoma from toxoplasma encephalitis in AIDS patients. AJNR Am J Neuroradiol **15**: 1885-1894, 1994.
6. Young RJ, Ghesani MV, Kagetsu NJ, Derogatis AJ. Lesion size determines accuracy of thallium-201 brain single-photon emission tomography in differentiating between intracranial malignancy and infection in AIDS patients. AJNR Am J Neuroradiol **26**: 1973-1979, 2005.
7. Lewitschnig S, Gedela K, Toby M, et al. ^{18}F-FDG PET/CT in HIV-related central nervous system pathology. Eur J Nucl Med Mol Imaging **40**: 1420-1427, 2013.
8. Westwood TD, Hogan C, Julyan PJ, et al. Utility of FDG-PETCT and magnetic resonance spectroscopy in differentiating between cerebral lymphoma and non-malignant CNS lesions in HIV-infected patients. Eur J Radiol **82**: e374-e379, 2013.
9. Mikita K, Maeda T, Ono T, Miyahira Y, Asai T, Kawana A. The utility of cerebrospinal fluid for the molecular diagnosis of toxoplasmic encephalitis. Diagn Microbiol Infect Dis **75**: 155-159, 2013.
10. Matsuura J, Fujii A, Mizuta I, Norose K, Mizuno T. Cerebral toxoplasmosis diagnosed by nested-polymerase chain reaction in a patient with rheumatoid arthritis. Intern Med **57**: 1463-1468, 2018.
11. Porter SB, Sande MA. Toxoplasmosis of the central nervous system in the acquired immunodeficiency syndrome. N Engl J Med **327**: 1643-1648, 1992.
12. Bargalló J, Berenguer J, García-Barrionuevo J, et al. The "target sign": is it a specific sign of CNS tuberculoma?. Neuroradiology **38**: 547-550, 1996.
13. Patkar D, Narang J, Yanamandala R, Lawande M, Shah GV. Central nervous system tuberculosis: pathophysiology and imaging findings. Neuroimaging Clin N Am **22**: 677-705, 2012.
14. Wasay M, Kheleani BA, Moolani MK, et al. Brain CT and MRI findings in 100 consecutive patients with intracranial tuberculoma. J Neuroimaging **13**: 240-247, 2003.
15. Hardy TA, Miller DH. Baló's concentric sclerosis. Lancet Neurol **13**: 740-746, 2014.
16. Licho R, Litofsky NS, Senitko M, George M. Inaccuracy of Tl-201 brain SPECT in distinguishing cerebral infections from lym-

phoma in patients with AIDS. Clin Nucl Med **27**: 81-86, 2002.

17. Rohren EM, Provenzale JM, Barboriak DP, Coleman RE. Screening for cerebral metastases with FDG PET in patients undergoing whole-body staging of non-central nervous system malignancy. Radiology **226**: 181-187, 2003.